JOC The Journal of Organic Chemistry

ARTICLE

pubs.acs.org/joc

Photooxidation of *n*-Octanal in Air: Experimental and Theoretical Study

Jovan M. Tadić,[†,*] Lai Xu,[‡] K. N. Houk,[‡] and Geert K. Moortgat[§]

[†]NASA Ames Research Center, Moffett Field, California 94035, United States

[‡]Department of Chemistry and Biochemistry, University of California, Los Angeles, California 90095, United States

[§]Max-Planck-Institut für Chemie, Atmospheric Chemistry Department, Postfach 3060, 55020 Mainz, Germany

Supporting Information

ABSTRACT:

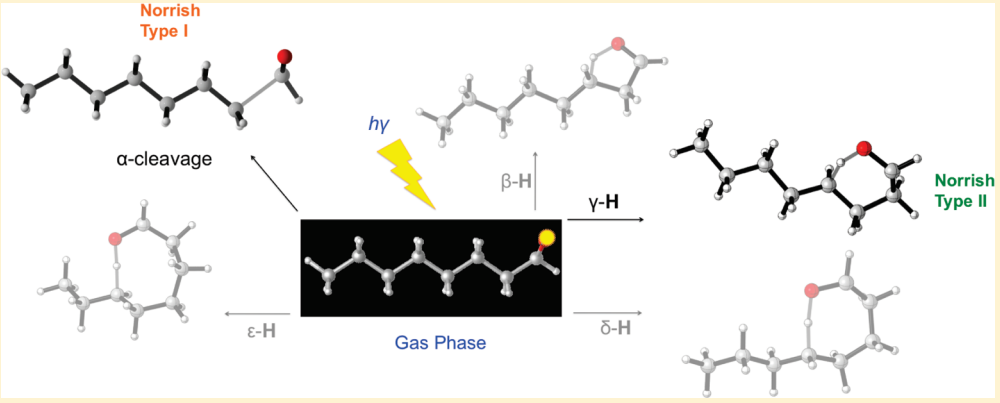

Dilute mixtures of *n*-octanal in synthetic air (up to 100 ppm) were photolyzed with fluorescent UV lamps (275−380 nm) at 298 K. The main photooxidation products were 1-hexene, CO, vinyl alcohol, and acetaldehyde. The photolysis rates and the absolute quantum yields were found to be slightly dependent on the total pressure. At 100 Torr, $\Phi_{100} = 0.41 \pm 0.06$, whereas at 700 Torr the total quantum yield was $\Phi_{700} = 0.32 \pm 0.02$. Two decomposition channels were identified: the radical channel $C_7H_{15}CHO \rightarrow C_7H_{15} + HCO$ and the molecular channel $C_7H_{15}CHO \rightarrow C_6H_{12} + CH_2{=}CHOH$, having absolute quantum yields of 0.022 and 0.108 at 700 Torr. The product $CH_2{=}CHOH$ tautomerizes to acetaldehyde. Carbon balance data lower than unities suggest the existence of unidentified decomposition channel(s) which substantially contributes to the photolysis. On the basis of experimental and theoretical evidence, *n*-octanal photolysis predominantly proceeds to form Norrish type II products as the major ones.

INTRODUCTION

Photodissociation of aldehydes represents an important source of free radicals in the lower atmosphere and thus may significantly influence the atmospheric oxidation capacity.[1] *n*-Hexanal and higher aldehydes have been observed in ambient air and in emissions of various plants, especially grasses, with comparable emissions rates as the monoterpenes.[2] The examination of longer chain aldehydes has recently come into the research focus, providing quantum yield and decomposition patterns data necessary for atmospheric modeling.[3−9] This is the first reported study on the photolysis of *n*-octanal.

Aliphatic aldehydes exhibit a weak absorption band in the wavelength range 240−360 nm as a result of a symmetry forbidden n−π^* transition.[10,11] There have been a number of studies devoted to the photodissociation of the simplest alkyl aldehydes, such as HCHO, CH_3CHO, and C_2H_5CHO,[12−20] and a recently growing number devoted to longer chain aldehydes, such as C_3H_7CHO, C_4H_9CHO,[3,21] isopentanal and *tert*-pentanal,[5] *n*-hexanal,[6,7] and *n*-heptanal.[7−9]

n-Hexanal and *n*-heptanal photodissociation patterns[6−9] and reaction schemes for *n*-pentanal[3] suggest that processes 1 and 2 play an important role in the photolysis of longer chain aldehydes:

$$n\text{-octanal} + h\nu \rightarrow \underset{\text{(Norrish type I)}}{n\text{-}C_7H_{15} + HCO} \quad (1)$$

$$\rightarrow \underset{\text{(Norrish type II)}}{C_6H_{12} + [CH_2 = CHOH]} \quad (2)$$

Process 1 represents the fragmentation into free radicals, with an enthalpy of around 350 kJ/mol, corresponding to a photochemical threshold of around 340 nm.[3] Process 2, which is

Received: November 9, 2010
Published: February 14, 2011

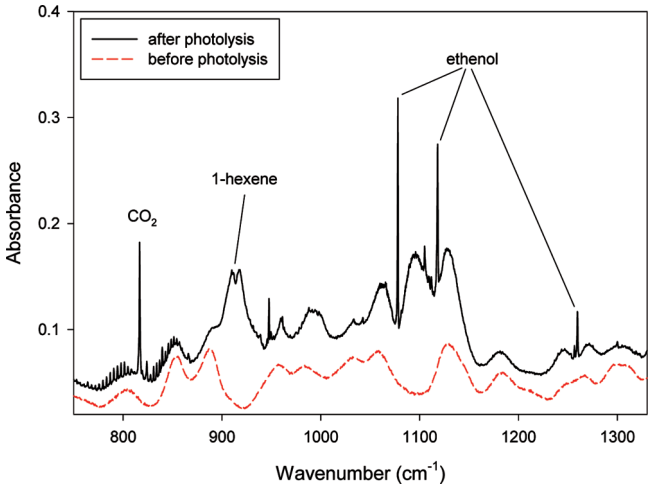

Figure 1. FTIR spectrum of 100 mTorr *n*-octanal, before and after photolysis (6 TL/12 lamps, 100 Torr synthetic air). Major products 1-hexene, ethenol, and CO_2, which is formed as a byproduct, are marked (exact positions of the peaks are given in the text).

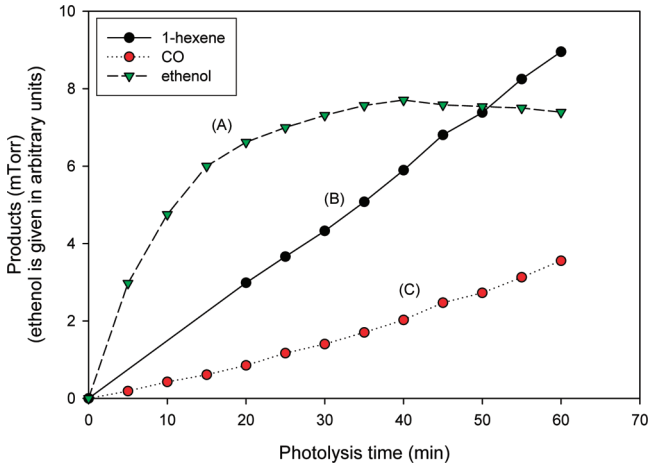

Figure 2. Photolysis of *n*-octanal−time profile: variation of the partial pressures of products. Curve of CO (C) shows that CO is not only the primary product but also a product of the reactions following a primary step. Ethenol partial pressure reaches maximum and then decreases by conversion to acetaldehyde.

common to molecules with a γ-hydrogen atom, is an intramolecular rearrangement with enthalpy around 80 kJ/mol ($\lambda \leq 1454$ nm).[3] The enthalpy change for process 2 was calculated assuming that the keto form of acetaldehyde is formed in the primary step. This assumption is not correct, and therefore, the enthalpy change for this reaction should be adjusted for the difference between the heats of formation of enol and keto forms of acetaldehyde (the equilibrium constant for keto−enol equilibrium is 5×10^{-6}, and the corresponding ΔG value is ~70 kJ/mol).[22] The total contribution of the Norrish I and II processes in the cases of *n*-butanal, *n*-pentanal, *n*-hexanal, and *n*-heptanal photolysis is, however, less than 100%, indicating a further reaction pathway (the calculation is made on carbon balance data).[4,6,9]

In this paper, the results obtained from the photolysis of small quantities of *n*-octanal in air, using wide band emission lamps, are reported together with theoretical investigation of the reactions of triplet aldehyde that results from photoexcitation using density functional theory. We have investigated the products and absolute quantum yields in the pressure range 100−700 Torr.

RESULTS AND DISCUSSION

The photooxidation experiments were carried out in a long-path quartz cell with detection of precursors and products by FTIR spectroscopy. After identification and quantification of the products, a mechanistic description of the photooxidation/photolysis is proposed. From the measured decay rate of the starting material, and from the knowledge of the absorption spectrum, overall quantum yields for the photolysis were calculated for various pressures.

Figure 1 shows the FTIR spectra of a mixture of 100 ppm *n*-octanal in synthetic air, before and after the photolysis. Major products observed are CO ($\nu_{max} = 2037-2235$ cm^{-1}), 1-hexene (880−940, 970−1012, 1420−1500, 1620−1660, 2810−3030, 3087.5 cm^{-1}), ethenol (vinyl alcohol, which is the enol form of acetaldehyde) (947.6, 1078, 1118.3, 1259.8 cm^{-1}), and acetaldehyde (1348.5−1355.5 cm^{-1}).

Figure 2 shows the concentration−time profiles for two products used for the estimation of Norrish type I/II absolute yields and their ratios. The only peak of 1-hexene that does not interfere with other present compounds, and which was used for the quantification, is fairly weak, resulting in a large uncertainty in the 1-hexene concentration at the beginning of the photolysis, and the first two points have been omitted from the plot.

1-Hexene is formed exclusively as a primary product in the reaction. Acetaldehyde is secondary product arising from ethenol conversion, and it undergoes further photolysis, which was described in our previous work on *n*-pentanal.[4] This time, only the identification of acetaldehyde was done.

Norrish type I reaction gives two radicals, which immediately react with oxygen. One of the products, formyl radical HCO, is quantitatively converted to CO and HO_2,[12,23,24] according to

$$HCO + O_2 \rightarrow HO_2 + CO \quad (3)$$

This process is followed through the rate of production of CO (2094−2096 cm^{-1}). The *n*-heptyl radicals are oxidized forming *n*-heptylperoxy radicals

$$n\text{-}C_7H_{15} + O_2 + M \rightarrow n\text{-}C_7H_{15}O_2 + M \quad (4)$$

The $n\text{-}C_7H_{15}O_2$ radicals subsequently react with HO_2, recombine, or disproportionate to produce a variety of products (reactions 5−8).[25,26]

$$n\text{-}C_7H_{15}O_2 + HO_2 \rightarrow n\text{-}C_7H_{15}OOH + O_2 \quad (5)$$

$$2n\text{-}C_7H_{15}O_2 \rightarrow 2n\text{-}C_7H_{15}O + O_2 \quad (6)$$

$$\rightarrow n\text{-}C_7H_{15}OH + n\text{-}C_6H_{13}CHO + O_2 \quad (7)$$

$$n\text{-}C_7H_{15}O + O_2 \rightarrow n\text{-}C_6H_{13}CHO + HO_2 \quad (8)$$

However, because of the estimated low reaction rate constant for the recombination and disproportionation, reactions 6 and 7,[26] the major expected product is *n*-heptyl hydroperoxide ($n\text{-}C_7H_{15}OOH$). This peroxide was not observed in the FTIR spectrum. Either its concentrations were under the detection limit (~1 mTorr) or the signals interfered with those of other compounds. No evidence of *n*-heptanal produced via channels 7 and 8 was observed.

1-Hexene is a stable molecular species and was used to calculate the rate of the Norrish type II process. The coproduct of the

dx.doi.org/10.1021/jo102133m |*J. Org. Chem.* 2011, 76, 1614–1620

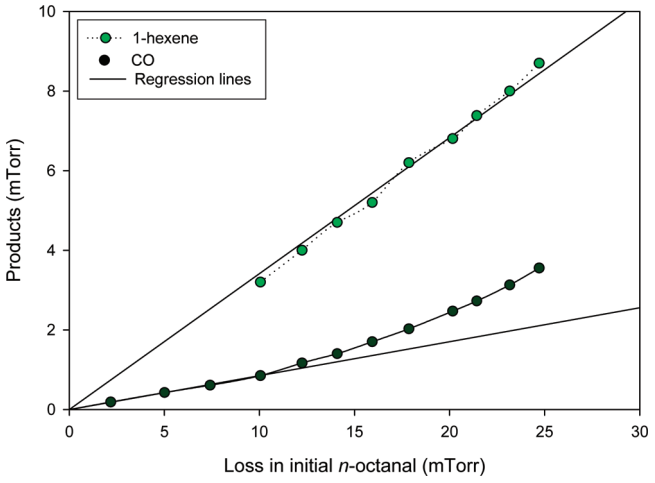

Figure 3. Photolysis of *n*-octanal products formed versus loss in *n*-octanal. See comments in the Figure 2 caption.

reaction is ethenol CH_2=CHOH, which tautomerizes slowly to acetaldehyde. This is clearly seen in Figure 2, where the peak integral−time profile of the enol product displays the behavior of a primary product involved in a secondary reaction. Ethenol concentration reaches a maximum after ∼40 min photolysis, and its subsequent decay is caused by its conversion to acetaldehyde.

Figure 3 shows profiles of product concentrations (partial pressures) of CO and 1-hexene versus loss of *n*-octanal.

According to the suggested mechanism, the yield of 1-hexene should be identical to the sum of the yields of ethenol and acetaldehyde, since all compounds are products of the same decomposition channel. CO originating from the reaction of HCO radical with oxygen can be treated as a primary product, but an increase in the yield at long conversion times is observed, which can be attributed to the photolysis of secondary products such as acetaldehyde, *n*-heptanal, etc. Theoretically, another possible source of CO could be the reaction

$$\underset{n\text{-octanal}}{n\text{-}C_8H_{16}O} + h\nu \rightarrow \underset{n\text{-heptane}}{n\text{-}C_7H_{16}} + CO \qquad (9)$$

The stable product of this reaction, *n*-heptane, was not identified in our experiments. Decarbonylation was not observed in the recent similar investigation of *n*-heptanal photolysis.[8] The relative probability for *n*-octanal molecules to undergo two detected decomposition channels is shown in Table 1. The probability is deduced from the ratio of primary formed CO (Norrish type I) and 1-hexene (Norrish type II).

Assuming that the formation of CO_2 is an artifact, the sum of both processes Norrish type I and II is 41 ± 7%, indicating the presence of other unidentified product channels.

n-Octanal molecules could undergo photocyclization, forming *cis/trans* isomers of 2-butylcyclobutanol (Scheme 1). This mechanism is observed in the photolysis of *n*-pentanal[27] and some ketones[7] and suggested as the important one in the photolysis of *n*-heptanal accounting for ∼30% of the total product yields.[8] These compounds were not detected in our experiments.

Absolute Quantum Yields. One of the objectives of the study was to determine the dependence of the absolute quantum yield on the total pressure. *n*-Butanal was used as the actinometer, with absolute quantum yields recently reported.[4] From the decay of *n*-octanal concentration (partial pressure), the photolytic rate constants were deduced for the different pressures by plotting

Table 1. Relative Probabilities for *n*-Octanal Molecule To Undergo Different Decomposition Channels (Errors Are Represented by Experimental Scatter)

total pressure (torr)	Norrish type I	Norrish type II
100	15.46	84.54
100	16.93	83.07
100	16.92	83.08
300	16.96	83.04
300	17.33	82.67
300	16.93	83.07
500	15.81	84.19
500	18.18	81.82
500	20.03	79.97
700	15.04	84.96
700	17.22	82.78
700	18.28	81.72
average	17.1 ± 3.0	82.9 ± 3.0

Scheme 1. Pathway to *Cis/Trans* Isomers of 2-Butylcyclobutanol

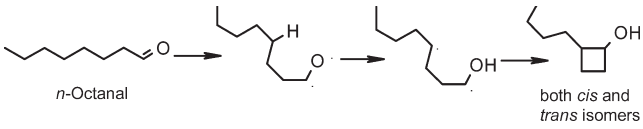

the natural logarithm of concentration versus time (first order decay) and performing a least-squares fit. From these results, overall quantum yields were calculated according to eq 10 using the overlap integrals of *n*-octanal and *n*-butanal spectra (integral equals unity) within the range of the TL/12 emission (275−380 nm).

$$\Phi^{int}(C) = \frac{K_{phot}(C)}{K_{phot}(OV)\dfrac{\Sigma OV(C)}{\Sigma OV(Act) \times \Phi^{int}(Act)}} \qquad (10)$$

In all cases, the absolute quantum yield dependency on the total pressure was observed. Measurements of all *n*-alkanal cross sections from C_2−C_9 have been performed recently by Zabel et al.[28] This study reveals that the UV spectra of the aldehydes from *n*-butanal upward are practically identical.

The absolute quantum yields data are summarized in Table 3 for all experiments performed at total pressures of 100, 300, 500, and 700 Torr and are also shown in form of the Stern−Volmer plot in Figure 4.

Since the intercept at zero pressure is not equal to 1 (the intercept is 2.4 ± 0.1), which should be the case if collisional deactivation was the only relaxation process besides the photodecomposition, it seems very probably that there are other energy-dissipating processes (the triplet state of *n*-octanal could deactivate by phosphorescence, etc.).[6] The interaction of the photoexcited molecules with the walls, resulting in the relaxation to the ground state, is of minor importance because of the huge volume-to-surface ratio of the reaction cell. The slope of the fitting line, described by $(1.061 \times 10^{-3})P$, corresponds to the sensitivity of absolute quantum yield on the total pressure P (in Torr).

The total quantum yield Φ^{tot} can be calculated from the following eq $1/\Phi^{tot} = 2.368 + (1.061 \times 10^{-3})P$. Using the

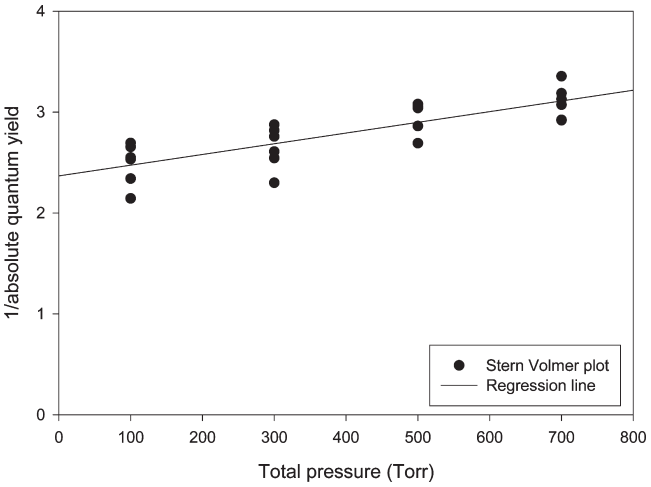

Figure 4. Pressure dependency of 1/(absolute quantum yields) in *n*-octanal photolysis at different total pressures of synthetic air (Stern−Volmer plot).

estimated absolute yield from Table 2 and quantum yield value from Table 3, it is possible to calculate the absolute contribution at atmospheric conditions (700 Torr): for Norrish type I (radical) process, $\varphi(\mathrm{I}) = 0.022 \pm 0.002$ and Norrish type II (molecular) $\varphi(\mathrm{II}) = 0.108 \pm 0.002$ (total quantum yield being 0.32, and a contribution of both decomposition channels being 41 ± 7%).

Comparison with other aldehydes (Table 3) shows that *n*-pentanal, *n*-hexanal, *n*-heptanal, and *n*-octanal have similar dependencies on the total pressure of synthetic air.[4,6,9] The sensitivity of the quantum yield on the total pressure (Torr) is described by the slope of the curve in Stern−Volmer plot and was 1.061×10^{-3}, 1.169×10^{-3}, 4.758×10^{-4}, 7.771×10^{-4}, and 1.931×10^{-3} for *n*-octanal, *n*-heptanal, *n*-hexanal, *n*-pentanal, and *n*-butanal, respectively.[4,6,9] *n*-Octanal is more or less in the line of *n*-heptanal, *n*-hexanal, and *n*-pentanal; *n*-butanal sensitivity is somewhat higher, which also accompanied with the substantially different Norrish type I/II ratio. This may point to the different spin-state distributions upon the photoexcitation.

Future work on the photolysis of the longer chain aldehydes should concentrate on the determination of the spin states of photoexcited molecules as precursors of Norrish type I and II processes and on the analysis of other possible products, since ∼60% of the initial aldehyde cannot be accounted for by Norrish type I and II reaction mechanisms. There is no conclusive evidence for the formation of cyclobutanol derivatives, and further examination of the subject should be performed. Possible examinations of the absolute quantum yield dependency on the low pressures of pure oxygen may reveal new information. The triplet ground electronic state of oxygen means that reaction pathways proceeding from the lowest triplet of the aldehyde (T_1) would be probably quenched more efficiently than the ones proceeding from the vibrationally excited ground singlet (S_0^*) or eventually from the first excited singlet (S_1). Thus, a stronger dependence of the decomposition parameters on oxygen pressure may be observed.

The main degradation processes of carbonyl compounds are controlled by photolysis and by the reaction with OH radicals. The atmospheric lifetime of *n*-octanal can be estimated from the knowledge of the OH reaction rate constant and the photodissociation rate. Unfortunately, the rate constant for OH reaction is not available. The rate constants for the OH reactions

Table 2. Absolute yields of Norrish Type I and II Decomposition Products in *n*-Octanal Photolysis (Errors Represent the Experimental Scatter)

total pressure (Torr)	Norrish type I (Δprimary CO/-Δoctanal)	Norrish type II (Δ1-hexene/-Δoctanal)
100	6.34	34.66
100	6.94	34.06
100	6.95	34.06
300	6.95	34.05
300	7.11	33.89
300	6.94	34.06
500	6.48	33.55
500	7.45	32.79
500	8.21	34.83
700	6.17	34.83
700	7.06	33.94
700	7.49	33.51
Average	7.01 ± 0.84	34.02 ± 0.81

of the homologous aldehydes, *n*-butanal,[29,30] *n*-pentanal,[27] and *n*-hexanal[6] were estimated to be 2.35×10^{-11}, 2.7×10^{-11}, and 1.9×10^{-11} cm^3 $molecule^{-1}$ s^{-1}, respectively. Although no data on the rate constant of *n*-octanal OH reaction is available, it is expected to be in line with these measurements, resulting in the reactive lifetime of 5−7 h under atmospheric conditions (average noontime OH concentration of 2×10^6 molecules cm^{-3} was used).

Maximum daytime photolysis rates for *n*-butanal and *n*-pentanal were estimated during in situ measurements in the photochemical outdoor reactor,[27] as $k_{ph,b} = (1.0 \pm 0.2) \times 10^{-5}$ s^{-1} for *n*-butanal and $k_{ph,p} = (1.6 \pm 0.15) \times 10^{-5}$ s^{-1} for *n*-pentanal, corresponding to a photolytic lifetime of 28 and 17 h, respectively. Our previous work on other homologous aldehydes and this study reveals similar behavior of *n*-octanal, *n*-heptanal,[9] *n*-hexanal,[6] and *n*-pentanal[4] photolysis parameters under laboratory conditions, including absolute quantum yield values, sensitivity on total pressure, and Norrish type I/II ratio. This would indicate that the dominant removal process in the lower troposphere for *n*-octanal, as for other homologous aldehydes, is the reaction with OH radicals but that photolytic processes still take some part in the degradation.

The absolute radical yield at atmospheric conditions can be estimated for *n*-octanal as 7.01 × 0.32 = 2.2%. If quantum yields for aldehydic compounds values are not known (e.g., for the use in atmospheric modeling), it is common to assume that they are unity, which is seldom the case as shown in this, and previous studies.[3−6,27] This often leads to an overestimation of the calculated radicals produced by photolysis.

Theoretical Studies. The optimized structures (triplet *n*-octanal, transition structures, and selected biradicals) of importance for hydrogen abstraction and α-cleavage are shown in Scheme 2, along with the zero-point energy corrected barrier heights (in kcal/mol). In comparing the feasibility of the carbonyl oxygen to extract a *β*-, *γ*-, *δ*-, or *ε*-hydrogen, it is clear that the highest barrier heights correspond to the five- and eight-membered ring transition structures (*β*- and *ε*-H). The five-membered TS involves significant angle strain to achieve the hydrogen-transfer geometry, while some unfavorable torsional interactions destabilize the eight-membered TS. Furthermore, α-cleavage is also a high-energy process, relative to *γ*- and *δ*-hydrogen abstraction, involving a 11.2 kcal/mol barrier height.

Table 3. Absolute Quantum Yield Values in *n*-Octanal, *n*-Heptanal,[9] *n*-Hexanal,[6] *n*-Pentanal[4] and *n*-Butanal[4] Photolysis at Different Pressures of Synthetic Air (Errors Are Represented by Experimental Scatter)

	absolute quantum yield				
total pressure (Torr)	*n*-octanal	*n*-heptanal[9]	*n*-hexanal[6]	*n*-pentanal[4]	*n*-butanal[4]
100		0.39			
100		0.35			
100	0.40	0.33			
100	0.47	0.41			
100	0.37	0.45			0.47
100	0.43	0.37	0.43	0.40	0.50
100	0.38	0.42	0.41	0.44	0.47
100	0.39	0.40	0.44	0.36	0.47
average	0.41 ± 0.06	0.39 ± 0.06	0.43 ± 0.02	0.40 ± 0.04	0.48 ± 0.02
300	0.44	0.38			
300	0.35	0.36			
300	0.35	0.36			
300	0.39	0.41	0.41	0.37	0.44
300	0.38	0.41	0.42	0.39	0.44
300	0.36	0.36	0.43	0.36	0.43
average	0.38 ± 0.06	0.38 ± 0.03	0.42 ± 0.01	0.38 ± 0.02	0.44 ± 0.01
500		0.32			
500	0.37	0.32			
500	0.33	0.32			
500	0.35	0.37	0.38	0.36	0.30
500	0.32	0.33	0.43	0.36	0.37
500	0.33	0.37	0.41	0.33	0.37
average	0.34 ± 0.03	0.32 ± 0.05	0.40 ± 0.03	0.35 ± 0.02	0.35 ± 0.05
700	0.34	0.31			
700	0.34	0.30			
700	0.33	0.31			
700	0.31	0.31	0.40	0.35	0.32
700	0.32	0.29	0.37	0.34	0.33
700	0.30	0.31	0.37	0.33	0.32
average	0.32 ± 0.02	0.31 ± 0.02	0.38 ± 0.02	0.34 ± 0.01	0.32 ± 0.01

Scheme 2. Different Reactive Channels from the Triplet State of *n*-Octanal (Box) Showing the Transition Structures and Relative Energies (in kcal/mol)[a]

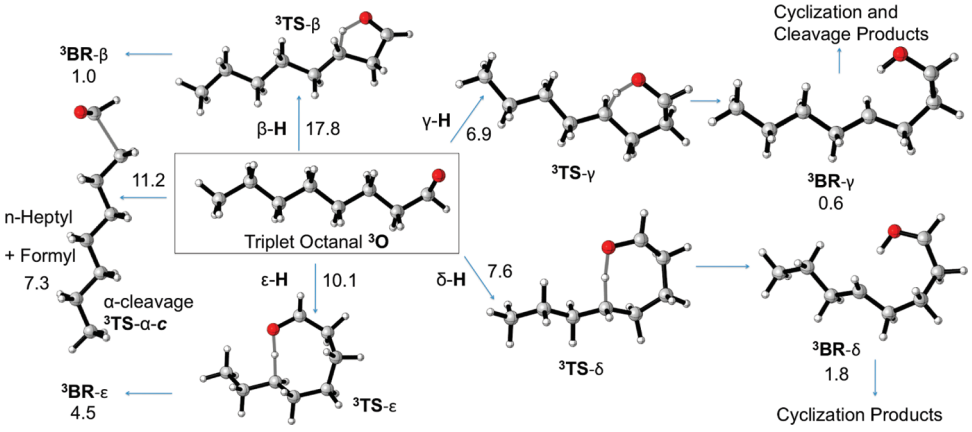

[a] Triplet biradicals generated by γ-H and δ-H abstraction are also shown.

Although γ-hydrogen abstraction has the lowest barrier height (6.9 kcal/mol), the transition structure for δ-H abstraction lies only 0.7 kcal/mol above the γ-H channel. Both of these TSs involve transition states with almost perfect chairlike

dx.doi.org/10.1021/jo102133m |J. Org. Chem. 2011, 76, 1614–1620

arrangements of the heavy atoms in the six- and seven-membered transition structures.

We also calculated the relative energies of the cyclized biradicals **3BR-γ** and **3BR-δ** and ground-state products formed by cyclization of these biradicals. The biradicals are slightly higher in energy than the triplet aldehyde, but rapid intersystem crossing to the singlet and cyclization is expected to occur. The relative energies of the *cis*- and *trans*-cyclopentanols (from cyclization of **3BR-δ**) are −65.7 and −65.9 kcal/mol, respectively. The cleavage of the **3BR-γ** yields 1-pentene and hydroxyethylene at a relative energy of −35.5 kcal/mol. Furthermore, the cyclization of **3BR-γ** yields the *cis*- and *trans*-cyclobutanols at relative energies of −48.7 and −51.4 kcal/mol, respectively.

The theoretical prediction of a high barrier for the Norrish type I reaction does not agree with the significant amount of this reaction observed experimentally. The α-cleavage may possibly also occur from the singlet state.

The results of the theoretical investigation are in good agreement with experimental findings in terms of importance of Norrish type II channel. Another channel very likely to occur, δ-H abstraction pathway, is not detected in our experiments. The lack of standards and the limitations of our experimental method prevented the detection of possible products of this channel—derivatives of cyclopentanol. Such products were postulated in other similar experiments with *n*-heptanal.[8]

CONCLUSIONS

Whereas simple aldehydes with up to four carbons undergo photochemical decomposition by Norrish type I reactions to form formyl and alkyl radicals,[4,6,27] higher aldehydes mainly decompose by the Norrish type II reaction, forming vinyl alcohol and the corresponding 1-alkene. Our study of *n*-octanal photolysis shows that the Norrish type II reaction is favored over the type I reaction. Theoretical calculations also show that the Norrish type II channel is favored. However, the decrease of the absolute yields of Norrish type I and II processes indicates that other, so far unidentified, processes become more and more important in the photolysis of longer chain aldehydes.

EXPERIMENTAL SECTION

The apparatus employed in this work has been described elsewhere[31,32] and will be briefly discussed here. The central part of the apparatus is a 44.2 L (1.40 m length and 20 cm diameter) quartz cell equipped with two independent sets of White-optic mirror arrangements. Sapphire-coated aluminum mirrors were used in the infrared region (l = 33.6 m) for the measurements of the educts and products. Infrared spectra at 0.5 cm^{-1} resolution (450−4000 cm^{-1}) were measured with a Bomem DA8-FTIR spectrometer. This method provides the possibility of simultaneous detection and monitoring of all the IR-active products and the starting material. Photolysis was achieved with six radially mounted lamps, TL/12-sunlamps (Philips 40W TL/12 lamps (275−380 nm). Spectra were taken every 5−10 min with a total irradiation time of 30−50 min. The extent of the conversion of initial compound was approximately 30%.

Experiments were carried out at room temperature (298 K) at pressures between 100 and 700 Torr (1 Torr = (101325/760)Pa), with an initial concentrations of approximately 100 ppm. Qualitative and quantitative data evaluation was carried out by comparing the product spectra with reference spectra obtained in the same cell and using calibration curves at corresponding pressures and resolution. Carbonyl compounds were obtained from a commercial supplier with purity higher than 98%. Before use, all samples were degassed by several freeze−pump−thaw cycles. The purity of the compounds was checked by FTIR spectral measurements, and no impurities were found. The calibration of vinyl alcohol was done indirectly, from the amount of formed acetaldehyde and the converted vinyl alcohol (peak decrease), since the conversion of these compounds is 1:1 (keto−enol tautomerism) according to

$$CH_2 = CH\text{-}OH \leftrightarrow CH_3\text{-}CH{=}O$$

Quantum Mechanical Methods. Quantum mechanical calculations were carried out using the Gaussian 09 suite of programs.[33] Density functional theory at the UB3LYP/6-31G* level of theory was used to obtain structure and energetic information along the triplet-state reaction coordinate.[34−36] All relative energies reported are zero-point energy (ZPE) corrected. Vibrational frequency calculations were also used to confirm that minimum energy structures have no imaginary frequencies, and transition structures (TS) have the appropriate imaginary frequency for α-cleavage (type I) or H-abstraction (type II).

ASSOCIATED CONTENT

Supporting Information. Cartesian coordinates and reference. This material is available free of charge via the Internet at http://pubs.acs.org.

AUTHOR INFORMATION

Corresponding Author
*E-mail: jotadic@lycos.com.

ACKNOWLEDGMENT

J.M.T. is supported by the NASA Senior Postdoc Program, Oak Ridge Associated Universities.

REFERENCES

(1) Graedel, T. E.; Farrow, L. A.; Weber, T. A. *Atmos. Environ.* **1976**, *10*, 1095. Grosjean, D. *Environ. Sci. Technol.* **1982**, *16*, 254. Finlayson-Pitts, B. J.; Pitts, J. N. *Atmospheric Chemistry*; John Wiley: New York, 1986.

(2) Owen, S.; Boissard, R.; Street, R. A.; Duckam, S. C.; Csiky, O.; Hewitt, C. N. *Atmos. Environ.* **1997**, *31* (S1), 101. Kirstine, W.; Galbally, I. *J. Geophys. Res.*, **1998**, *103*, 10603.

(3) Cronin, J. T.; Zhu, L. *J. Phys. Chem. A* **1998**, *102*, 10274.

(4) Tadić, J.; Juranić, I.; Moortgat, G. K. *J. Photochem. Photobiol. A: Chem.* **2001**, *5817*, 1.

(5) Zhu, L.; Cronin, J. T.; Narang, A. *J. Phys. Chem. A* **1999**, *103* (36), 7248.

(6) Tadić, J.; Juranić, I.; Moortgat, G. K. *Molecules* **2001**, *6*, 287.

(7) Tang, Y.; Zhu, L. *J. Phys. Chem. A* **2004**, *108* (40), 8307.

(8) Paulson, S.; Liu, D.-L.; Orzechowska, G.; Campos, L. M.; Houk, K. N. *J. Org. chem.* **2006**, *71* (17), 6403.

(9) Tadić, J.; Juranić, I.; Moortgat, G. K. *J. Chem. Soc. Perkin Trans. 2* **2002**, 135.

(10) Calvert, J. G.; Pitts, J. N. *Photochemistry*; John Wiley; New York, ; p 372.

(11) Lee, E. K. C.; Lewis, R. S. *Adv. Photochem.* **1980**, *12*, 1.

(12) Moortgat, G. K.; Seiler, W.; Warneck, P. *J. Chem. Phys.* **1983**, *78*, 1185.

(13) Carmely, Y.; Horowitz, A. *Int. J. Chem. Kin.* **1984**, *16*, 1585.

(14) Moore, C. B.; Weishaar, J. C. *Annu. Rev. Phys. Chem.* **1983**, *34*, 525.

(15) Ho, P.; Bamford, D. J.; Buss, R. J.; Lee, Y. T.; Moore, C. B. *J. Chem. Phys.* **1982**, *76*, 3630.

(16) Horowitz, A.; Calvert, J. G. *J. Phys. Chem.* **1982**, *86*, 3105.
(17) Meyrahn, H.; Moortgat, G. K.; Warneck, P. Presented at the 15th Informal Conference on Photochemistry, Stanford, CA, July, 1982.
(18) Shepson, P. B.; Heicklen, J. *J. Photochem.* **1982**, *19*, 215.
(19) Heicklen, J.; Desai, J.; Bahta, A; Harper, C.; Simonaitis, R. *J. Photochem.* **1986**, *34*, 117.
(20) Terentis, A. C.; Knepp, P. T.; Kable, S. H. *J. Phys. Chem.* **1995**, *99*, 12704.
(21) Forgeter, S.; Berces, T; Dobe, S *Int. J. Chem. Kinet.* **1979**, *11*, 219.
(22) Guthrie, J. P.; Cullimore, P. A. *Can. J. Chem.* **1979**, *57*, 240.
(23) Horowitz, A.; Calvert, J. G. *Int. J. Chem. Kinet.* **1978**, *10*, 805.
(24) Horowitz, A.; Su, F.; Calvert, J. G. *Int. J. Chem. Kinet.* **1978**, *10*, 1099.
(25) Atkinson, R. *J. Phys. Chem. Ref. Data*, **1994**, Monograph 2.
(26) Lightfoot, P. D.; Cox, R. A.; Crowley, J. N.; Destriau, M.; Hayman, G. D.; Jenkin, M. E.; Moortgat, G. K.; Zabel, F. *Atmos. Environ.* **1992**, *26A*, 1805.
(27) Moortgat, G. K. Final report on EU project RADICAL: "Evaluation of radical sources in atmospheric chemistry through chamber and laboratory studies"; ENV4-CT97-0419, March 2000.
(28) Zabel, F. Reaktionswege von Alkoxyradikalen unter atmosphärischen Bedingungen und UV-Absorptionsspektren von Carbonylverbindungen. In Becker, K.H., Coordinator; Annual report 1998 on BMBF-project TFS/LT3, FKZ 07TFS30, 1999, p 69.
(29) Semmes, D. H.; Ravishankara, H. R.; Gump-Perkins, C. A.; Wine, P. H. *Int. J. Chem. Kinet.* **1985**, *17*, 303.
(30) Kerr, J. A.; Sheppard, D. W. *Environ. Sci. Technol.* **1981**, *15*, 960.
(31) Moortgat, G. K.; Cox, R. A.; Schuster, G.; Burrows, J. P.; Tyndall, G. S. *J. Chem. Soc., Faraday Trans. II* **1989**, *85*, 809.
(32) Raber, W. H.; Moortgat, G. K. In *Advanced Series in Physical Chemistry, 3, Progress and Problems in Atmospheric Chemistry*; Barker, J. R., Ed.; World Scientific Publ. Co.: Singapore, 1995; p 318.
(33) Gaussian 09, Revision A.1: Frisch, M. J.; Trucks, G. W.; Schlegel, H. B.; Scuseria, G. E.; Robb, M. A.; Cheeseman, J. R.; Scalmani, G.; Barone, V.; Mennucci, B.; Petersson, G. A.; Nakatsuji, H.; Caricato, M.; Li, X.; Hratchian, H. P.; Izmaylov, A. F.; Bloino, J.; Zheng, G.; Sonnenberg, J. L.; Hada, M.; Ehara, M.; Toyota, K.; Fukuda, R.; Hasegawa, J.; Ishida, M.; Nakajima, T.; Honda, Y.; Kitao, O.; Nakai, H.; Vreven, T.; Montgomery, J. A., Jr.; Peralta, J. E.; Ogliaro, F.; Bearpark, M.; Heyd, J. J.; Brothers, E.; Kudin, K. N.; Staroverov, V. N.; Kobayashi, R.; Normand, J.; Raghavachari, K.; Rendell, A.; Burant, J. C.; Iyengar, S. S.; Tomasi, J.; Cossi, M.; Rega, N.; Millam, J. M.; Klene, M.; Knox, J. E.; Cross, J. B.; Bakken, V.; Adamo, C.; Jaramillo, J.; Gomperts, R.; Stratmann, R. E.; Yazyev, O.; Austin, A. J.; Cammi, R.; Pomelli, C.; Ochterski, J. W.; Martin, R. L.; Morokuma, K.; Zakrzewski, V. G.; Voth, G. A.; Salvador, P.; Dannenberg, J. J.; Dapprich, S.; Daniels, A. D.; Ö. Farkas, Foresman, J. B.; Ortiz, J. V.; Cioslowski, J.; Fox, D. J. Gaussian, Inc., Wallingford, CT, 2009.
(34) Becke, A. D. *J. Chem. Phys.* **1993**, *98*, 5648.
(35) Krishnan, R.; Binkley, J. S.; Seeger, R.; Pople, J. A. *J. Chem. Phys.* **1980**, *72*, 650.
(36) Head-Gordon, M.; Pople, J. A. *Chem. Phys. Lett.* **1988**, *153*, 503.